Fizika Nizkikh Temperatur, 1996, v. 22, No 2, p. 174–181

Heat transfer in solid parahydrogen with heavy impurities (neon, argon)

V. G. Manzhelii, B. Ya. Gorodilov, and A. I. Krivchikov

B. Verkin Institute for Low Temperature Physics and Engineering, National Academy of Sciences of Ukraine, 47 Lenin Ave., 310164, Kharkov, Ukraine
E-mail:manzhelii@ilt.kharkov.ua

1. Introduction

Heavy impurities strongly scatter phonons and distort the low-frequency part of the energy spectrum of a crystal [1]. This must considerably affect the thermal conductivity of crystals at low temperatures [2,3].

The choice of solid parahydrogen as a matrix was dictated by the following considerations:

1. The mass ratio of an impurity particle and the hydrogen molecule M_i / M_m is always large, implying a strong impurity influence on thermal conductivity. For the Ne–H_2 and Ar–H_2 systems this ratio is 10 and 20, respectively.

2. Parahydrogen can be prepared to a high degree of purity with a concentration of nonhydrogen impurities below 0.1 ppm. It is comparatively easy to obtain high quality parahydrogen single crystals with minimum content of defects [4]. These facts and the large values of M_i / M_m allow one to study impurity effects at very low impurity concentrations. In turn, this makes it possible to get information about normal phonon-phonon processes which is difficult to determine by other methods. In a very pure, perfect, and rather large crystal, normal phonon-phonon processes dominate at low temperatures. With increasing impurity concentration, the intensity of resistive processes goes up. Information about the normal phonon-phonon processes can be obtained from thermal conductivity measurements in the case when the relaxation rates of normal and resistive processes are comparable [5–7].

3. Solid parahydrogen is an insulating crystal with central intermolecular interaction. Heat transfer in solid parahydrogen is performed solely by phonons. This makes the interpretation of the results easier.

Ne and Ar whose atoms have no low-energy internal degrees of freedom were chosen as impurities.

2. Experiment

Gaseous hydrogen used in the experiments was purified from chemical impurities and partly from isotopic impurities with a palladium filter. The concentration of orthohydrogen was 0.21%. The chemical purities of neon and argon (natural isotopic composition) were 99.99%. The errors in the concentration of neon and argon in the mixtures did not exceed 15% of their quoted values.

The longitudinal steady-state heat flow method of thermal conductivity measurement was used [8]. Single crystals of the solutions were grown in a glass tube having a length of 75 mm and an inner diameter of 7 mm. The measurement technique is described in Ref. 8. At the first stage the crystals were obtained by directly condensing gaseous mixtures into the solid phase. During crystal growth the temperature of the ampoule bottom was steadily decreased with a cooling rate of 0.5 K/h. The crystallization temperature was regulated through the pressure of the gas fed, which was kept constant (about 30–40 Torr). The crystal was grown during 6 to 8 hours. The monocrystallinity of the samples was checked by inspection in polarized light. The crystals were grown both from the gas and liquid phases. The thermal conductivity of dilute solutions was independent of sample growth procedure. Random errors in thermal conductivity did not exceed 5%.

3. Ne–pH_2 and Ar–pH_2 weak solutions

At the first stage, the chosen impurity concentrations were very low so that we could avoid phase separation and neglect the direct interaction between the impurity atoms.

3.1. Ne–pH_2 *system* [8]

Parahydrogen and neon have very close parameters of intermolecular interaction potentials. It allows neon to be considered as a quasi-isotopic impurity in parahydrogen. Thermal conductivities of 6

© V. G. Manzhelii, B. Ya. Gorodilov, and A. I. Krivchikov, 1996

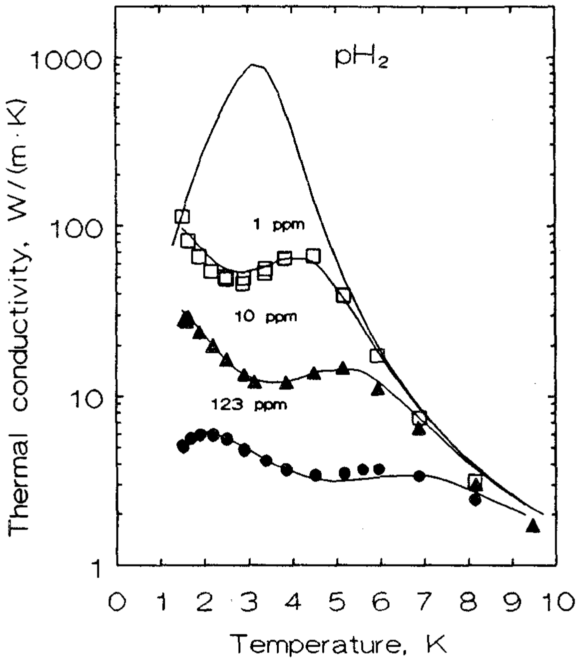

Fig. 1. Thermal conductivity of crystals of pure pH_2 and pH_2 with Ne impurity (the concentrations in ppm are indicated); the solid lines are calculated results.

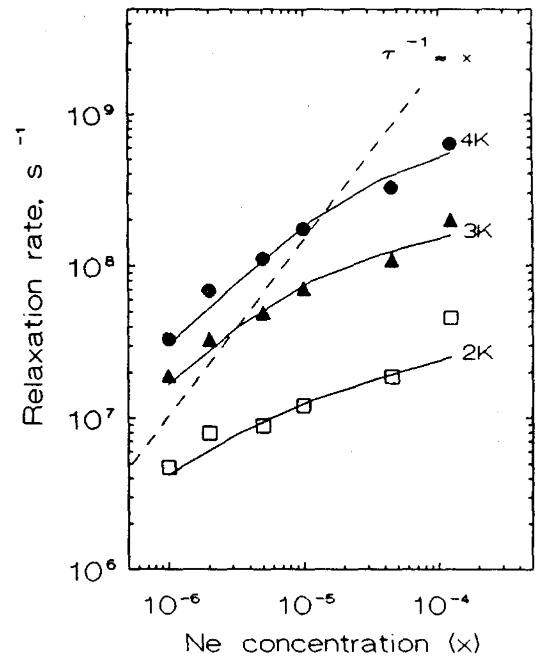

Fig. 2. Neon concentration dependence of the effective relaxation rate of phonons in Ne-doped solid pH_2 for different temperatures (the dashed line is a linear dependence $\tau^{-1} \sim x$).

solutions of neon in parahydrogen with neon concentrations from 1 to 123 ppm were measured in the temperature range 1.5 to 10 K. Figure 1 shows experimental temperature dependences of the thermal conductivity of the solutions with neon concentrations 1, 10, and 123 ppm. The thermal conductivity of pure parahydrogen is shown for comparison.

Three features attract attention in the behaviour of the thermal conductivity of the solid solutions.

First, the results obtained indicate an extremely strong effect of the neon impurity on the thermal conductivity. Near $T = 3$ K the neon impurity of concentration 1 ppm decreased the thermal conductivity of solid parahydrogen by an order of magnitude. The scattering cross section of the neon atom at a concentration of $x = 1$ ppm and $T = 3$ K is three orders of magnitude higher than that of an isolated pair of orthohydrogen molecules. This allowed us to disregard the conversion-promoted reduction of the orthohydrogen concentration in the samples below 0.21%. However, the magnitude of the effect itself is not surprising. Above all, the guest to host mass ratio is very high ($M_i / M_m = 10$). In addition, the impurity effect is observed near the thermal conductivity maximum of solid parahydrogen where the role of other resistive processes is minimal.

Second, it is worth noting that there is a minimum in the temperature dependence of the thermal conductivity, which shifts towards higher temperatures with increasing neon concentration. This is due to resonance scattering of phonons by quasi-local vibrations which appear in the crystal when heavy impurities are introduced.

Third, unusual is that at very low impurity concentrations the thermal resistivity and the phonon relaxation rate τ^{-1} as a function of the neon concentration are considerably weaker than linear. This is illustrated in Fig. 2, which shows the concentration dependence of the relaxation rate of phonons at temperatures 2, 3, and 4 K. The dashed line is a linear concentration dependence of τ^{-1}. To determine experimental values of the relaxation rate of phonons τ^{-1}, the gas-kinetic relationship was used for phonons:

$$\lambda = \frac{Cv^2\tau}{3} , \tag{1}$$

where C is the specific heat capacity [9]; v is the average sound velocity [10]. The unusual finding implies that impurity atoms separated on the average by a distance of about 100 lattice constants do not scatter phonons independently. This cannot be due to direct interaction between impurity atoms taking into account the short-range dispersion forces. The reason for the observed concentration dependence of the thermal resistivity is that the intensity of resistive processes is comparable with that of the normal phonon-phonon processes in parahydrogen in the temperature range studied. It is well known that normal processes by themselves do not produce thermal resistivity. However, in combination with resistive scattering processes, which depend on phonon frequency, the normal processes affect the magnitude of the thermal resistivity [7]. If the normal processes dominate (Ziman limit), they restore the quasi-equilibrium distribution of phonons between the successive acts of phonon scattering on impurities. In this case, the acts of phonon scattering by impurity particles are independent of each other, and the thermal resistivity is a linear function of the concentration. Otherwise, the dependence turns out to be weaker. It is this situation that is realized in the neon-parahydrogen solutions studied.

A quantitative description of the thermal conductivity behaviour became possible after the interference between normal phonon-phonon processes, Umklapp processes, resonance scattering of phonons by heavy impurities, and boundary scattering have been taken account [8]. The well-known model of Callaway was used [5]. Figures 1 and 2, which depict the temperature dependence of the thermal conductivity and the concentration dependence of the phonon relaxation rate, show good agreement between theoretical predictions and experimental data. The results of theoretical calculations are presented in Figs. 1 and 2 by solid curves. Expressions (2)–(5) were used to describe the phonon relaxation rates for various scattering mechanisms, which are:

resonance scattering

$$\tau_i^{-1}(\omega) = \frac{3/2\,\pi x \varepsilon^2 \omega (\omega/\omega_D)^3}{(1-\omega^2/\omega_0^2)^2 + 9/4\,\pi^2\varepsilon^2(\omega/\omega_D)^6}\,, \qquad (2)$$

where $\varepsilon = (M_i/M_m) - 1$; $\omega_0 = \omega_D/(3\varepsilon)^{1/2}$;

U-processes

$$\tau_U^{-1}(\omega) = A_U\,\omega^2 T\,e^{-U/T}\;; \qquad (3)$$

boundary scattering

$$\tau_b^{-1} = v/l = 1\cdot 10^6\ \mathrm{s}^{-1}\;, \qquad (4)$$

where l is the mean free path of phonons;

normal processes

$$\tau_N^{-1}(\omega) = A_N\,\omega^2 T^3\;. \qquad (5)$$

The effective phonon relaxation rate was described by the expression:

$$\tau_{\mathrm{eff}} = \langle\tau_t\rangle + \frac{\langle\tau_t/\tau_N\rangle^2}{\langle 1/\tau_N\rangle - \langle\tau_t/\tau_N^2\rangle}\,, \qquad (6)$$

where $\tau_t^{-1} = \tau_N^{-1} + \tau_{\mathrm{res}}^{-1}$; $\tau_{\mathrm{res}}^{-1} = \tau_i^{-1} + \tau_U^{-1} + \tau_b^{-1}$.

The parameters of Umklapp processes ($A_U = 2.45\cdot 10^{-15}$ s/K) and the boundary scattering were estimated using experimental data on the thermal conductivity of pure parahydrogen [4]. Equation (5) for normal processes was obtained for temperatures

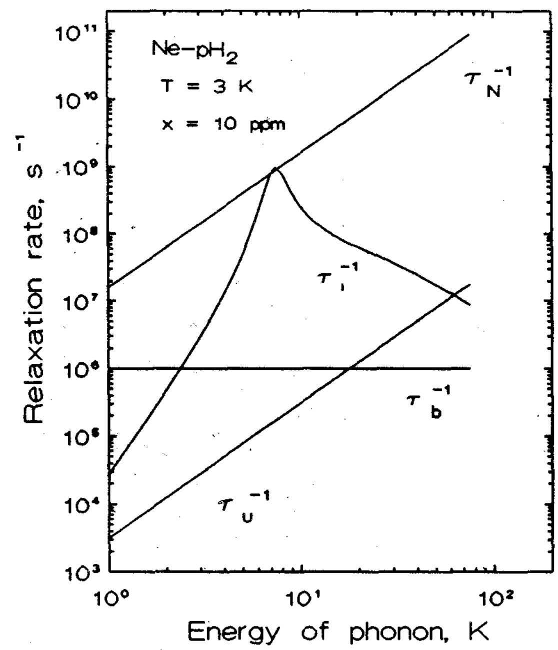

Fig. 3. The phonon relaxation rate vs. phonon energy for different scattering processes: N-processes (τ_N^{-1}); impurity scattering (τ_i^{-1}); boundary scattering (τ_b^{-1}); U-processes (τ_U^{-1}).

essentially below the Debye temperature. Such a consideration is true for the whole region of existence of quantum crystals, in which the Debye temperatures are much higher than the melting points. The numerical coefficient A_N was estimated through fitting Eq. (6) to experimental results to be $3.8\cdot 10^{-18}$ s/K^3.

Let us now discuss in more detail the role of different phonon scattering mechanisms. Figure 3 is a plot of the phonon relaxation rate versus the phonon energy for different scattering mechanisms at a neon concentration of $x = 10$ ppm and $T = 3$ K. Under the conditions mentioned, the interference of the normal processes and the processes of phonon resonance scattering by impurities is of main importance. An increase or decrease in the neon concentration will respectively increase or decrease the relaxation rate due to phonon scattering by impurities. As the temperature increases, the role of the Umklapp processes increases. With decreasing temperature, the role of the boundary scattering grows. Figure 4 shows the concentration dependence of the effective phonon relaxation rate τ_{eff}^{-1} at 2 K. The quantity τ_{eff}^{-1} was calculated with an account of the interference of normal and resonance scattering processes. As one can see, the Ziman limit, at which $\tau_{\mathrm{eff}}^{-1} \sim x$, occurs only at neon concentrations of the order 10^{-7} and lower. At such concentrations, however, the boundary scattering processes (or Umklapp processes at higher tempera-

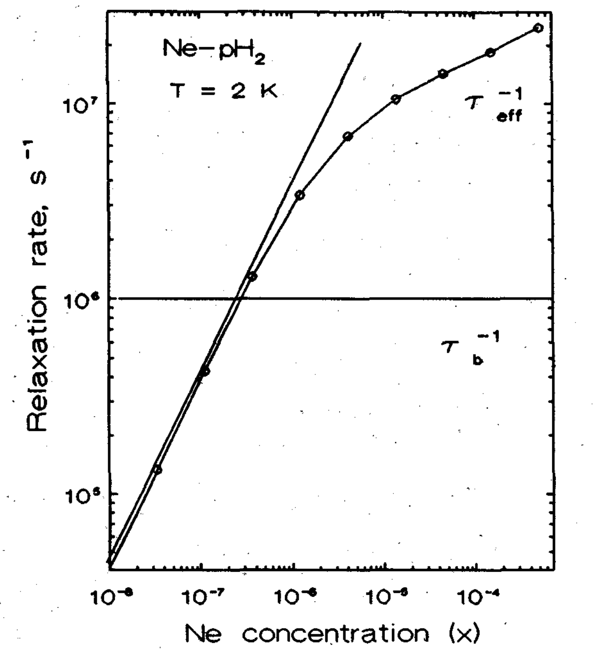

Fig. 4. Ne concentration dependence of the effective relaxation rate of phonons in doped solid pH_2 ; $\tau_{\rm eff}^{-1}$ is the effective relaxation rate of phonons; τ_b^{-1} is the relaxation rate for boundary scattering; the straight line is $\tau^{-1} \sim x$.

tures) dominate. Thus, in Ne–pH$_2$ solutions, the Ziman limit is not reached even at the smallest neon concentration ($1 \cdot 10^{-6}$) used in experiments and it is necessary to take the interference of normal and resistive scattering processes into consideration.

Figure 5 presents the temperature dependence of the relaxation rates for different resistive processes at a neon concentration of $x = 10$ ppm. It also shows the effective relaxation rate obtained with allowance for the interference of normal and resistive processes and, in addition, the Ziman limit curve ($\tau_N << \tau_{\rm res}$). As was already noted, at low temperatures the boundary scattering plays an important role while Umklapp processes dominate at high temperatures. At the same time, the interference of normal and resonance scattering processes should be taken into account in the whole temperature range studied. The contribution of the resonance scattering processes is especially large because it is proportional to the second power of the mass defect $\varepsilon = (M_i / M_m) - 1$ (see Eq. (2)). One can also see that the Ziman limit is not reached in the larger part of the temperature range studied.

We focus our attention on the degree of deviation from the Ziman limit since the information about normal processes can be obtained from thermal conductivity measurements only in the case when the deviation mentioned is reasonably high. As known, it is rather difficult to obtain this information by other methods. For this reason the system used by us is unique. For comparison, Fig. 6 shows temperature dependences of the phonon relaxation rates for a solution of Ne in ^{4}He (the mass ratio $M_i / M_m = 5$). The calculations were made by us using the results

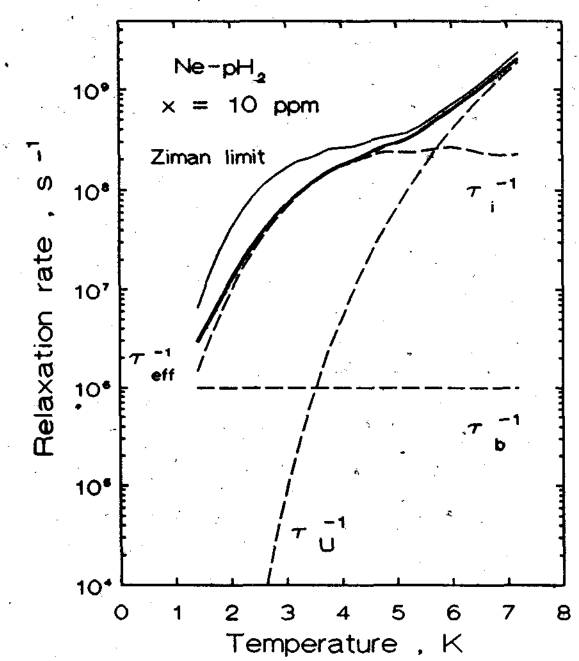

Fig. 5. Temperature dependence of the phonon relaxation rate for different scattering processes in the Ne–pH$_2$ system: the solid lines are the effective relaxation rates. The upper curve corresponds to the Ziman limit ($\tau_{\rm res} >> \tau_N$).

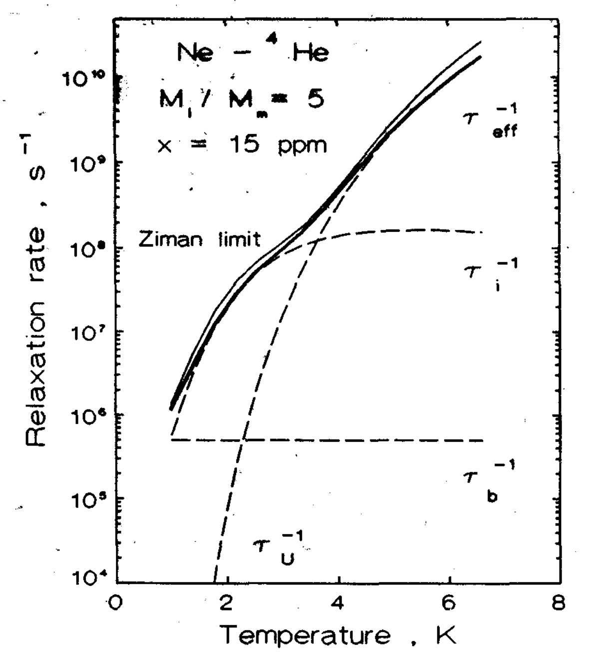

Fig. 6. Temperature dependence of the phonon relaxation rate for different scattering processes in the Ne–^{4}He system: the solid lines are the effective relaxation rates. The upper curve corresponds to the Ziman limit ($\tau_{\rm res} >> \tau_N$).

derived from thermal conductivity studies of the Ne–^{4}He solutions obtained by Berman and Livesley [11]. As seen, the deviation from the Ziman limit is comparatively small even in this system for which the mass ratio is rather large.

Investigation of thermal conductivity and phonon scattering processes in quantum crystals is of special interest. Introduction even of a heavy isotope impurity into a quantum crystal must be accompanied by a change of the force constants and a dilatation of the lattice in the vicinity of the impurity particle [12]. These effects, in principle, must affect the resonance scattering of phonons by impurities [3]. We have not managed to find such an influence on the thermal conductivity of solid solutions of Ne in $p\mathrm{H}_2$. Even in the case of Ne in ^{4}He solutions [11], these effects turned out to be small and were effectively taken into account through varying the impurity to host mass ratio within 20%. As known, quantum crystals are strongly anharmonic and this must lead to an increased phonon-phonon interaction and a growth of the intensity of normal processes. However, the extremely poor experimental information about normal processes and the low accuracy of determination of their parameters do not allow any conclusion to be drown about normal processes in quantum crystals.

3.2. Ar–$p\mathrm{H}_2$ *system* [13]

As the next step, it seemed natural to investigate the effect of nonisotopic heavy impurities with central interaction on the thermal conductivity of solid parahydrogen. Argon was chosen as the impurity. In this case, two factors affect the thermal conductivity of the solution; namely, the very large impurity to host mass ratio ($M_i/M_m = 20$) and the substantial difference between the interaction potentials of the impurity and the matrix. Thermal conductivities of solid solutions with argon concentrations of 0.4 and 1.3 ppm were measured in the temperature range 1.5 to 8 K.

Figure 7 shows experimental temperature dependences of the thermal conductivity of solutions of argon in parahydrogen, of pure parahydrogen, and of parahydrogen with 1 ppm neon impurity as well. A theoretical curve for the solution of Ar–$p\mathrm{H}_2$ at an argon concentrations of $x = 1.3$ ppm is also given for comparison. This curve is calculated assuming Ar to be an isotope impurity. One can see in Fig. 7 that the influence of argon on the thermal conductivity of parahydrogen is significantly weaker than that of neon in spite of the fact that in the case of argon impurities the mass ratio is twice as large. The results obtained were successfully described within the heat transfer model proposed by Antsygina and Slyusarev [14] for simple molecular crystals with heavy impurities. According to this model, impurity particles that interact strongly with the matrix scatter phonons considerably weaker than in the case of resonance scattering. The expression obtained by Antsygina and Slyusarev for the ultimately strong interaction of impurity particles with nearest neighbours (strong coupling) does not involve the intermolecular interaction parameters:

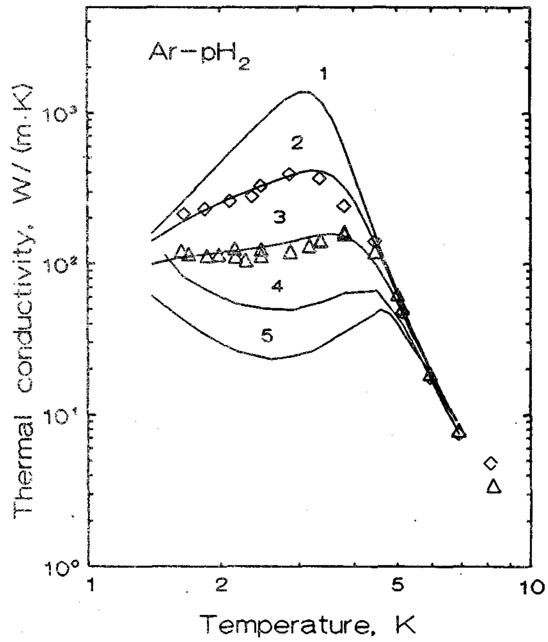

Fig. 7. Calculated and experimental data for the temperature dependence of the thermal conductivity: smoothed data for pure $p\mathrm{H}_2$ (*1*); theory (using Eq. (7)) (*2*, *3*); $p\mathrm{H}_2$ with: 0.4 ppm Ar (◇); 1.3 ppm Ar (△); 1.0 ppm Ne (*4*); theory for isotopic (using Eq. (2)) Ar impurity ($x = 1.3$ ppm) (*5*).

$$\tau_i^{-1}(\omega) = \frac{[1 + 2gP(\omega)]^2 R_2(\omega)}{[P(\omega) - R_1(\omega) - 2gP(\omega)R_1(\omega)]^2 + [1 + 2gP(\omega)]^2 R_2^2(\omega)}, \tag{7}$$

where $g = M_m/M_i - 1$. In the Debye approximation for the vibrational spectrum of the crystal, the functions $P(\omega)$, $R_1(\omega)$, and $R_2(\omega)$ have the form

$$P(\omega) = 1 - 1.5\omega/\omega_D + (\omega/\omega_D)^2 - $$
$$- 3(\omega/\omega_D)^3 \ln(1 + \omega_D/\omega) \ ,$$

$$R_1(\omega) = -1 - 1.5\omega/\omega_D - (\omega/\omega_D)^2 + \\ + 3(\omega/\omega_D)^3 \ln |\omega_D/\omega - 1| \ ,$$

$$R_2(\omega) = 3\pi(\omega/\omega_D)^3 \ .$$

Here, ω_D is the Debye frequency.

The results of the theoretical calculation using the expression are shown in Fig. 7 by solid lines. As one can see, in spite of the simplified and in many aspects unreal character of the theoretical model, it describes the experimental data suprisingly well. This gives impetus to discuss more closely the consequences of this model.

Figure 8 shows the relaxation rate vs. the phonon energy for different types of scattering (Rayleigh, resonance, and strong coupling). At the low energy end, the relaxation rates for all three types of phonon scattering coincide and are proportional to the fourth power of energy. The differences manifest themselves at energies close to the resonance (quasi-local) frequency. In the case of strong coupling, an initially monotonic weakening of the relaxation rate versus phonon energy dependence is observed, instead of a resonance peak. Then this dependence rapidly tends to zero after passing through a maximum. So, the contribution of argon impurity to the thermal resistivity of parahydrogen decreases sharply when the phonon energy increases. At present we cannot propose a convincing physical explanation of this result, which formally follows from theory.

The experimental data on thermal conductivity neither confirm nor disprove the theoretical predictions of a sharp weakening of the scattering of high-energy phonons by argon impurity. Figure 9 shows to what extent the experimental thermal conductivity data of a solution with 1.3 ppm of argon agree with theoretical estimates in the case when the phonon spectrum is cut off from above at various phonon energies. The theoretical curve describes experiment well already at a cutoff energy of $E_c = 20$ K. Further increase of this energy does not change noticeably the theoretical curve. It means that the impurity scattering of phonons with energies exceeding 20 K must manifest itself in the temperature range where the Umklapp processes dominate and impurity scattering is negligible.

4. Oversaturated Ne–pH$_2$ and Ar–pH$_2$ solutions [15]

According to up-to-date studies, the limiting solubility of neon in parahydrogen is close to $(1–2) \cdot 10^{-4}$ [15,16]. At reasonably rapid crystallization of the gas mixtures, one-phase nonequilibrium long-living solutions with concentrations exceeding the limiting solubility can be in principle obtained. We studied thermal con-

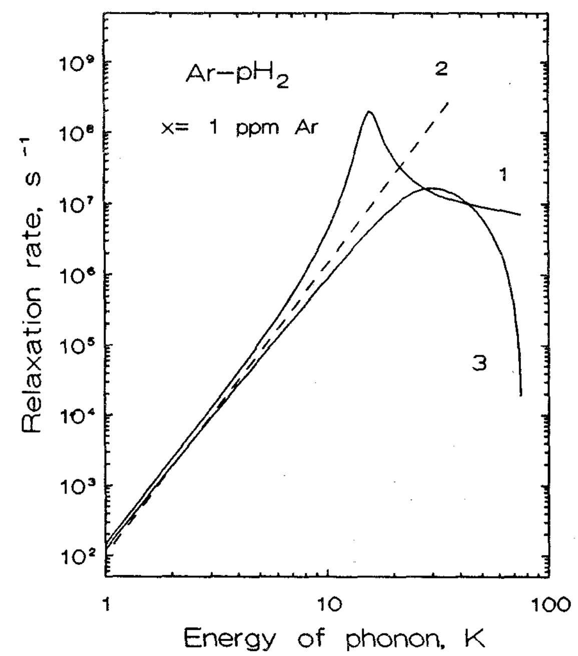

Fig. 8. Phonon energy dependence of the phonon relaxation rate for various types of phonon scattering by impurity: resonance (*1*), Rayleigh (*2*), and as obtained from the strong coupling model of Eq. (7) (*3*).

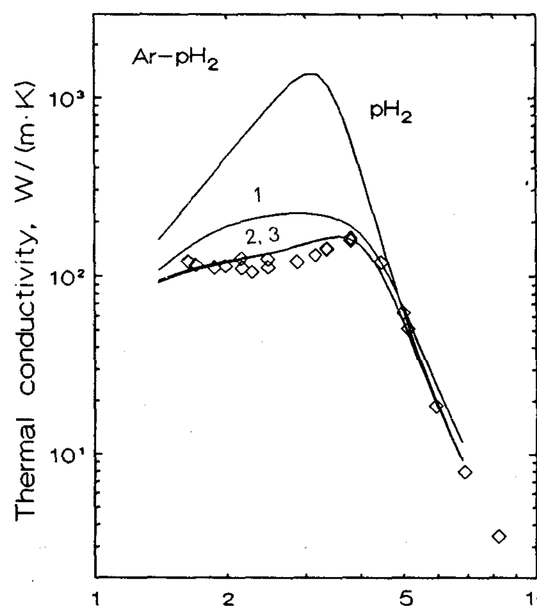

Fig. 9. Theoretical description of the thermal conductivity of the Ar–pH$_2$ solution with 1.3 ppm Ar for different cutoff energies of the phonon spectrum: 10 K (*1*); 20 K (*2*); 118 K (*3*) (Debye temperature). The upper curve is for pure p-H$_2$. The curves for 20 and 118 K are indistinguishable; ◇ — experimental data for pH$_2$ with 0.4 ppm Ar.

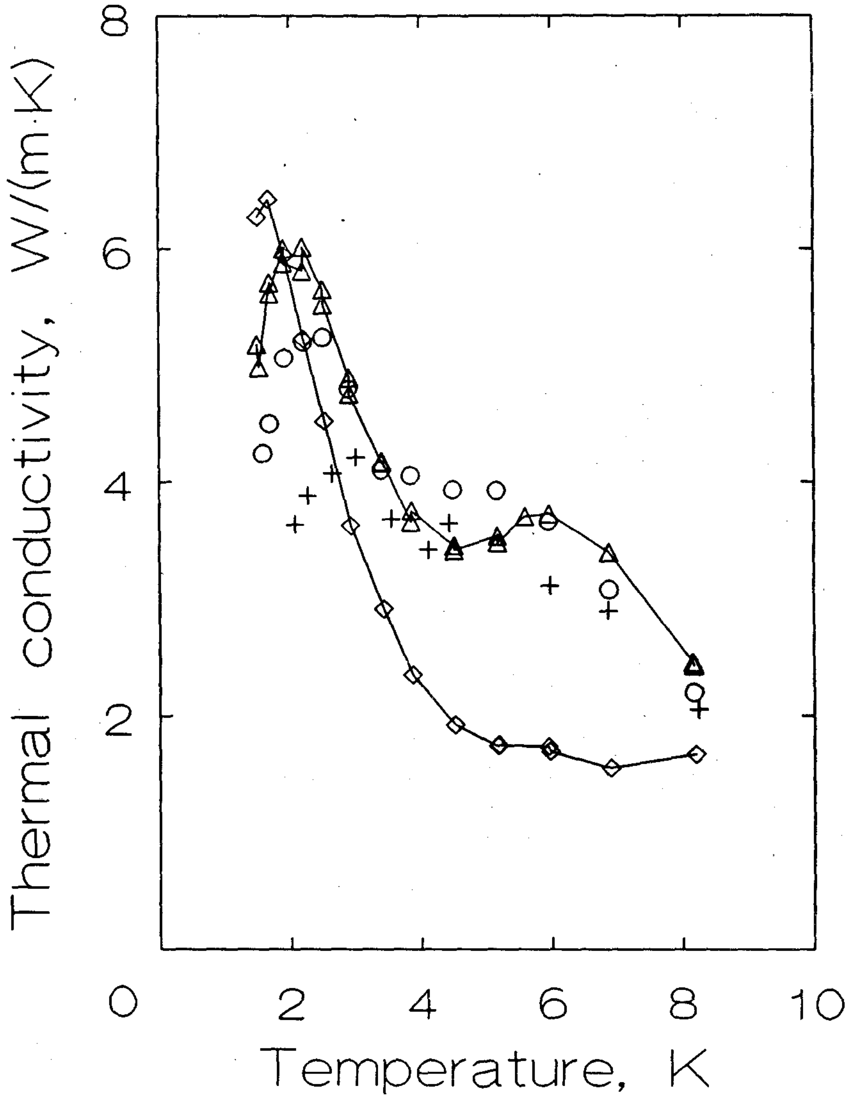

Fig. 10. Thermal conductivity of oversaturated solutions $(pH_2)_{1-x}Ne_x$ as function of temperature: x = 0.012% (△); 0.1% (◇); 0.5% (○); 1.3% (+).

ductivity of oversaturated Ne–pH_2 solutions with neon concentrations of $1\cdot10^{-3}$, $5\cdot10^{-3}$ and $1.3\cdot10^{-2}$. The results are shown in Fig. 10. The thermal conductivity of a weak solution with a neon concentration of $1.2\cdot10^{-4}$ is presented for comparison. When condensing the gas with a neon concentration of $1\cdot10^{-3}$ we managed to obtain an oversaturated one-phase solution. As it was expected, the thermal conductivity of this solution turned out to be lower than that of weak solutions with lower neon concentrations. For solutions with neon concentrations $5\cdot10^{-3}$ and $1.3\cdot10^{-2}$, the thermal conductivities above 3.5 K coincide within experimental error with the thermal conductivity of the solution with neon concentration $1.2\cdot10^{-4}$. We recall that the neon concentration in the last solution is close to the limiting solubility. It is natural to assume that increasing the neon concentration in the last two solutions leads to phase separation. After separation, the neon concentration in the weak solution of neon in parahydrogen appeared to be close to the limiting solubility. At low temperatures, the boundary scattering becomes noticeable. It may be implied that the boundary scattering is stronger for two-phase solutions. This explains the lower thermal conductivity of the phase separated solutions at temperatures below 3.5 K.

The limiting solubility of argon in solid parahydrogen is by two orders of magnitude lower than that of neon in pH_2. Similar results were obtained for oversaturated solutions of Ar in pH_2 (at argon concentrations 4.6 and 50 ppm).

The work described in this article has been made possible by support from the International Science Foundation, Grants U9R000 and U9R200.

1. Yu. Kagan and Ya. A. Iosilevskii, *Zh. Eksp. Teor. Fiz.* **45**, 819 (1964).
2. C. T. Walker and R. O. Pohl, *Phys. Rev.* **131**, 1433 (1963).
3. A. A. Maradudin, *Solid State Phys.* **18**, 273 (1966).
4. N. N. Zholonko, B. Ya. Gorodilov, and A. I. Krivchikov, *JETP Lett.* **55**, 167 (1992).
5. J. Callaway, *Phys. Rev.* **113**, 1046 (1959).
6. R. A. Guyer and J. A. Krumhansl, *Phys. Rev.* **148**, 766 (1966).
7. R. Berman, *Thermal conductivity in solids*, Claredon Press, Oxford (1992).
8. T. N. Antsygina, B. Ya. Gorodilov, N. N. Zholonko, A. I. Krivchikov, V. G. Manzhelii, and V. A. Slyusarev, *Sov. J. Low Temp. Phys.* **18**, 283 (1992).
9. M. I. Bagatskii, I. Ya. Minchina, and V. G. Manzhelii, *Sov. J. Low Temp. Phys.* **10**, 542 (1984)
10. V. G. Manzhelii and M. A. Strzhemechny, in: *Cryocrystals*, B. I. Verkin and A. F. Prikhot'ko (eds.) [in Russian], Naukova Dumka, Kiev (1983).
11. R. Berman and D. M. Livesley, *J. Phys.* **C14**, L945 (1981).
12. R. Berman, C. L. Bounds, C. D. Day, and H. H. Sample, *Phys. Lett.* **26A**, 185 (1968).
13. B. Ya. Gorodilov, A. I. Krivchikov, V. G. Manzhelii, and N. N. Zholonko, *Low Temp. Phys.* **20**, 66 (1994).
14. T. N. Antsygina and V. A. Slyusarev, *Low Temp. Phys.* **19**, 348 (1993).
15. B. Ya. Gorodilov, A. I. Krivchikov, V. G. Manzhelii, N. N. Zholonko, and O. A. Korolyuk, *Low Temp. Phys.* **21**, 723 (1995).
16. I. Ya. Minchina, M. I. Bagatskii, V. G. Manzhelii, and P. I. Muromtsev, *Low Temp. Phys.* **21**, 531 (1995).